Journal of Advanced Research in Fluid Mechanics and Thermal Sciences

Journal homepage:
https://semarakilmu.com.my/journals/index.php/fluid_mechanics_thermal_sciences/index
ISSN: 2289-7879

Investigation of Water Content and Minimum Droplet Temperature of Spray Drying Product with Inlet Temperature and Air Flow Direction Variation Using CFD Method

Eflita Yohana[1,*], Mohammad Tauviqirrahman[1], Eka Dharmawan[1], Mohamad Endy Julianto[2], Kwang-Hwan Choi[3], Luhung Damarran Achmad[1]

[1] Department of Mechanical Engineering, Faculty of Engineering, Diponegoro University, Jl. Prof. Soedarto, S.H., Semarang 50275, Indonesia
[2] Department of Chemical Engineering, Vocational School, Diponegoro University, Jl. Prof. Soedarto, S.H., Semarang 50275, Indonesia
[3] College of Engineering, Pukyong National University, 365 Sinseon-ro, Nam-gu, Busan 608739, Korea

ARTICLE INFO

Article history:
Received 5 February 2022
Received in revised form 25 April 2022
Accepted 28 April 2022
Available online 27 May 2022

Keywords:
Spray dryer; water content; droplet temperature

ABSTRACT

This study aimed to analyze the effect of inlet temperature and airflow direction variation of a spray dryer on the product's water content and minimum droplet temperature using the means of computational fluid dynamics (CFD). The airflow direction types were mixed and co-current. To simulate the flow, the k-ω SST and standard k-ε models were utilized, and the Eulerian-Lagrangian approach was used to estimate particle motion. The simulation results showed that water content reduced as temperature climbed for both airflow directions and vice versa for the minimum droplet temperature. With droplets diameters of 10 µm and 30 µm and an inlet temperature of 180°C, both mixed flow and co-current flow spray dryer generated the lowest water content (0%) output. The lowest minimum droplet temperature (32.73°C) occurred in the mixed flow spray dryer with an inlet temperature of 100°C.

1. Introduction

Spray drying is a product processing technique that involves converting liquid material into dry particles using a hot drying medium [1,2]. The drying rate and quality of the finished product are influenced by the spray dryer's operating conditions and product composition [1]. A spray dryer uses controlled operating conditions to achieve high drying air temperatures and fast drying durations while maintaining a low droplet temperature. These advantages make spray drying suitable for drying products that are highly sensitive to heat and maintain product qualities such as color, taste, and nutrition [3,4]. The spray drying method is widely chosen commercially also due to its ability to achieve lower production costs and drying time and high humidity reduction rates [5-8].

Spray drying is a common drying process for a variety of foods and health items, including instant coffee, powdered milk, tea, and vitamins [9,10]. The beverage prepared from dried tea leaves

* *Corresponding author.*
E-mail address: eflitayohana@live.undip.ac.id

https://doi.org/10.37934/arfmts.95.2.99112

(*Camellia sinensis*) is one of Asia's most popular beverages, with extensive studies of its benefits on human health. Tea leaves contain many beneficial ingredients, with bioactive compounds called polyphenols being one of the most critical groups, possessing rich antioxidant properties that can potentially prevent cancer and, more recently, an antiviral agent to treat COVID-19 [11-13].

The preservation of bioactive compounds in tea leaves is of utmost importance in the industry. Transforming tea leaves into powder form by spray drying technology proved beneficial, mainly in reducing product volume, prolonging shelf life, and retaining thermally sensitive compounds [14]. The use of the computational fluid dynamics (CFD) method to study the flow behavior throughout the drying process to optimize the design and minimize the cost of a spray dryer has become possible thanks to advances in computer technology. CFD method reduce time and cost compared to experimental method, while also give a more detailed and extensive fluid phenomenon compared to analytical observation [15]. Many experimental and numerical research have been conducted to investigate the properties of the spray drying process. CFD analyses showed good predictions of the temperature and velocity distributions in the spray dryer compared to the experimental approach [1,16-19].

Mainly, three basic types of air-droplets contact systems are applied in spray drying technology: co-current, countercurrent, and mixed [20]. The selection of contact systems of a spray dryer is crucial to avoid damage or loss of natural compounds that are thermolabile in the product. A co-current spray dryer is the most widely used spray dryer than a countercurrent spray dryer, with a mixed flow spray dryer as a good option to dry thermostable products [21]. Thus, the variations of airflow direction in this study are mixed flow and co-current flow. Many parameters determine the drying performance of a spray dryer, some of them are: drying air flow rate, fluid flow characteristics, and the drying air temperature.

Studies have shown the effect of drying air flow rate to the quality of the spray drying products. One study showed that increasing drying air flow rate would lead to effective drying of the particle and higher yield [22]. Another study confirmed this finding while also found that higher drying air flow rate caused an increase in outlet temperature, thus decreasing the moisture content of the dried product. Higher drying air flow rate results in a decrease in droplet diameters, creating a much more efficient spray drying conditions [23]. One study found that decreasing drying air flow rate results in higher energy efficiency, while increasing the drying air flow rate leads to higher energy savings. This is due to the fact that while energy supply to the spray dryer increases, the energy required for evaporation does not change. This causes more energy available in the exhaust air, allowing it to be recovered in an air-to-air heat exchanger [24].

Using a suitable turbulence model in a spray dryer simulation influences the accuracy of the airflow characteristics in the drying chamber [25]. The drying air inlet of the mixed flow spray dryer, which is placed at the upper edge of the drying chamber, is modified in this study. This modification causes the drying air to enter tangentially, creating a tendency to form a swirl-like flow in a cyclone separator. The k-ω SST turbulence model provides more accurate rotating flow modelling results than the k-ε turbulence model [26,27]. However, the standard k-ε turbulence model can produce more accurate fluid flow characteristics at the spray dryer wall compared to realizable k-ε and RNG k-ε turbulence models [1,16,28,29]. It has also been shown that while Reynolds Stress Model (RSM) turbulence model can provide more accurate results, the k-ω SST and the standard k-ε has a much lower computational time [17,30,31]. As a result, the mixed and co-current flow spray dryers are modelled using the k-ω SST and standard k-ε turbulence models, respectively.

The effect of temperature on the spray drying process has been studied extensively. High temperature drying air can result in lower water content and water activity in the product [32]. Several numerical and experimental studies have also shown that increasing the inlet temperature

of the drying air causes a rise in the outlet temperature, reducing the amount of water content within the product and shortening the drying time [33,34]. Droplet temperature can also provide vital information for the determination of drying kinetics, in which the increase of inlet temperature results in the increase of the minimum droplet temperature that exits the spray dryer [35,36].

Given the above descriptions, it has been shown that the spray dryer's inlet temperature affects the water content and minimum droplet temperature of the dried product. Thus, it is crucial to gain a deeper understanding of the inlet temperature and airflow direction variation of a spray dryer on the product's water content and minimum droplet temperature. This study aimed to do so utilizing the computational fluid dynamics (CFD) method.

2. Methodology

2.1 Governing Equation

A three-phase flow solution using the Eulerian-Lagrangian approach was used to estimate particle tracking the spray dryer in this work. The continuous phase in this approach is air, while the discrete phase is particles [16]. The gas phase was analyzed using the Eulerian approach by solving the Navier-Stokes equation, and the particle movement was simulated using Lagrangian path analysis. Drag and gravity are the forces that act on particles. Eq. (1) to Eq. (3) give the continuity, momentum, and energy equations for incompressible fluid flows.

$$\rho + \rho(\nabla . \vec{v}) = 0 \tag{1}$$

$$\rho \frac{D\vec{V}}{Dt} = -\nabla p + \rho \vec{g} + \mu\left(\nabla^2 \vec{V}\right) \tag{2}$$

$$\rho . c_{pf} . v . \nabla T = \nabla\left(\lambda_f . \nabla T\right) + \mu\phi \tag{3}$$

Individual particles in the stream were tracked using the discrete phase model (DPM). The particles in this spray dryer simulation are assumed to be spherical and non-rotating, with negligible particle interaction and no effect on the fluid flow field (one-way coupling). Therefore, the particle's motion equation can be written according to Eq. (4) and Eq. (5).

$$\frac{dx_p}{dt} = \vec{u}_p \tag{4}$$

$$\frac{d\vec{u}_p}{dt} = F_d\left(\vec{u} - \vec{u}_p\right) + \vec{g}_x \frac{(\rho_p - \rho)}{\rho_p} \tag{5}$$

Fluid velocity is $(\vec{u})$, particle velocity is $\left(\vec{u}_p\right)$, x_p denotes particle position, $\vec{g}_x$ is the gravitational force, ρ is the fluid density, and ρ_p denotes particle density. In Eq. (5), $F_d(\vec{u} - \vec{u}_p)$ denotes drag per unit mass of particles, where F_d can be calculated based on Eq. (6).

$$F_d = \frac{1}{\tau_p} \frac{(C_d - Re_p)}{24} \tag{6}$$

where $\left(\tau_p\right)$ is particle relaxation time, given by Eq. (7).

$$\tau_p = \frac{\rho_p d_p^2}{18\mu} \tag{7}$$

The drag coefficient (C_d) is a function of the particle's Reynolds number (Re_p). The value of the particle's Reynolds number is determined by Eq. (8) [28].

$$Re_p = \rho d_p \frac{|\vec{u}-\vec{u}_p|}{\mu} \tag{8}$$

For spherical particles, the drag coefficient is determined using Morsi and Alexander's [37] correlation, with values of a_1, a_2, and a_3 taken from the relative particle's Reynolds number (Re_p), as given by Eq. (9).

$$C_d = a_1 + \frac{a_2}{Re_p} + \frac{a_3}{Re_p} \tag{9}$$

The DPM uses the species transport model to forecast heat and mass transfer between drying air and particles during the drying process, as well as the temperature and water content of the dried product's particles. Eq. (10) can be used to write the heat transfer equation

$$\frac{d}{dt}\left(m_p c_p T_p\right) = hA_p\left(T_g - T_p\right) + \frac{dm_p}{dt} h_{fg} \tag{10}$$

where m_p denotes the mass of the particle, c_p is particle specific heat, T_p is the particle temperature, $h_{fg}$is the latent heat of vaporization, A_p is particle surface area, and h denotes the heat transfer coefficient.

A mass transfer rate equation is needed to determine the rate of evaporation of the particles when the temperature of the particles approaches the evaporation and the boiling point temperature. Eq. (11) calculates the rate of mass transfer (evaporation) between gas and particles

$$\frac{dm_p}{dt} = -k_c A_p\left(Y_s^* - Y_g\right) \tag{11}$$

where Y_s^* denotes the saturation humidity, Y_g is gas humidity, and k_c is the mass transfer coefficient.

The vapor concentration on the particle surface is determined in a spray drying process by assuming that the partial vapor pressure on the particle surface is equal to the saturated vapor pressure at the particle temperature. Eq. (12) calculates the vapor concentration in the drying air [16]

$$Y_g = X_i \frac{P_{op}}{RT_\infty} \tag{12}$$

where P_{op} is the operating pressure during the drying process. The mass transfer coefficient k_c in Eq. (11) can be obtained with the Sherwood number given by Eq. (13)

$$Sh = \frac{k_c d_d}{D_{i,m}} = 2.0 + 0.6 Re^{\frac{1}{2}} Sc^{\frac{1}{3}} \tag{13}$$

where Sh is the Sherwood number, Sc is the Schmidt number, $D_{i,m}$ is the diffusion coefficient, d_d is the diameter of the particle, and Re is the Reynolds number in Eq. (8).

After the particles dried with the spray dryer have reached their boiling point, the boiling rate of the model can be determined by Eq. (14) [38]

$$\frac{dd_p}{dt} = \frac{4k_{ta}}{\rho_p c_g d_p}\left(1 + 0.23\sqrt{Re}\, ln\left[1 + \frac{c_g(T_g - T_p)}{h_{fg}}\right]\right) \quad (14)$$

where k_{ta} is the thermal conductivity of the gas, with c_g being the specific heat capacity of the gas.

2.2 CFD Model

In this study, two spray dryer geometries were simulated, with differences in the direction of the air inlet of the dryer: the mixed flow spray dryer has the air inlet through the upper edge of the drying chamber, whereas the air inlet to a co-current flow spray dryer is in the direction of atomization. The governing equations were solved numerically using ANSYS Fluent. The SIMPLE scheme was utilized to obtain convergence in the pressure-velocity coupling. For pressure discretization, the second order scheme was adopted to accurately forecast the distribution of velocity and temperature under actual conditions. The momentum, dissipation rate, and kinetic energy discretization were all done using the first order upwind scheme. To reduce numerical instability and improve convergence, the first order upwind approach was employed to discretize the energy equation. All solution variables were subjected to $1x10^{-4}$ convergence requirements, while the energy equation was subjected to $1x10^{-6}$ convergence criteria.

2.2.1 Mixed flow spray dryer

The geometry of the mixed flow spray dryer was created using SOLIDWORKS software. The shape and geometric dimensions of the spray dryer are shown in Figure 1 and Table 1.

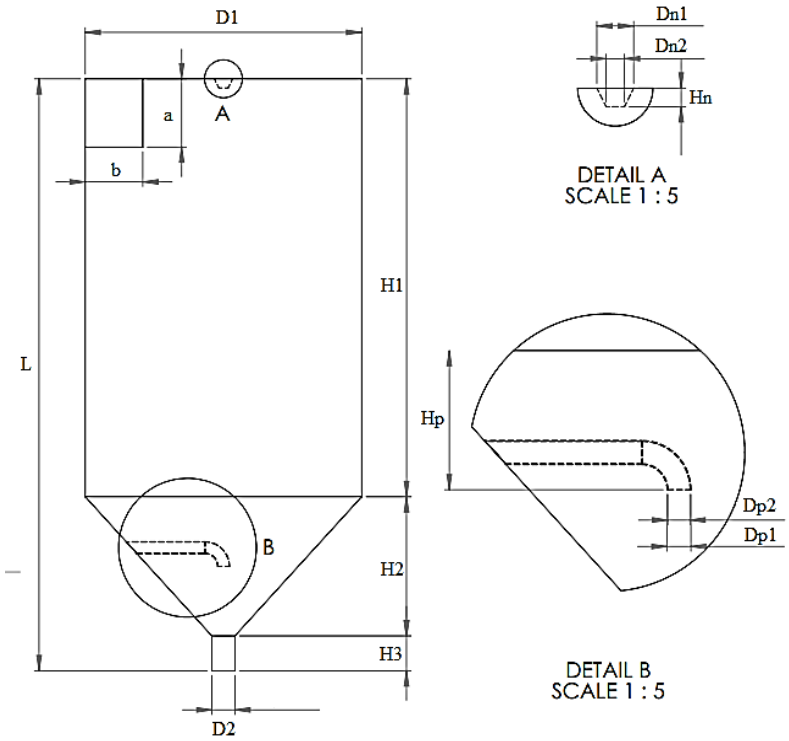

Fig. 1. Geometry of mixed flow spray dryer

Table 1
Dimensions of mixed flow spray dryer

Geometry	Dimension (mm)
Body diameter, D1	600
Cylinder diameter, D2	50
Nozzle diameter 1, Dn1	40
Nozzle diameter 2, Dn2	20
Pipe diameter 1, Dp1	26
Pipe diameter 2, Dp2	24
Inlet dimension, a×b	147×125
Cylinder height, H1	900
Cone height, H2	300
Cylinder height, H3	480
Nozzle height, Hn	20
Pipe to cylinder distance, Hp	150
Spray dryer length, L	1275

2.2.2 Co-current flow spray dryer

The co-current flow spray dryer design was based on the research of Anandharamakrishnan *et al.,* [1]. The geometry of the spray dryer was made using SOLIDWORKS software. The shape and geometric dimensions of the spray dryer are shown in Figure 2 and Table 2.

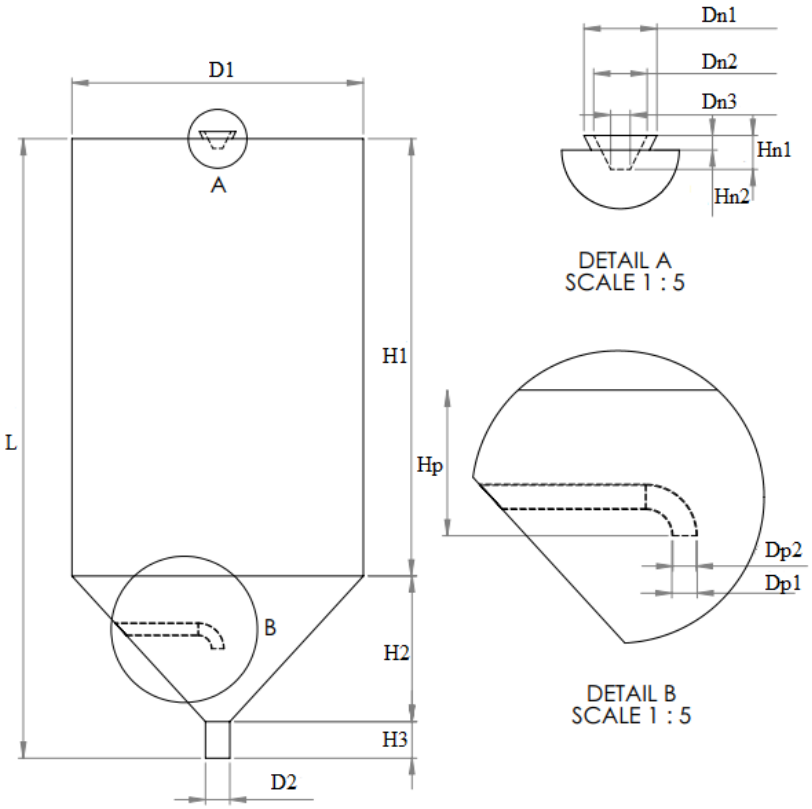

Fig. 2. Geometry of co-current flow spray dryer

Table 2
Dimensions of co-current flow spray dryer

Geometry	Dimension (mm)
Body diameter, D1	600
Cylinder diameter, D2	50
Nozzle diameter 1, Dn1	81
Nozzle diameter 2, Dn2	55
Nozzle diameter 3, Dn3	20
Pipe diameter 1, Dp1	26
Pipe diameter 2, Dp2	24
Cylinder height, H1	900
Cone height, H2	300
Cylinder height, H3	480
Nozzle height 1, Hn1	35
Nozzle height 2, Hn2	15
Pipe to cylinder distance, Hp	150
Spray dryer length, L	1275

2.3 Boundary Conditions

The inlet velocity and outlet pressure were the inlet and outlet boundary conditions, respectively. The spray dryer surface boundary condition was set to wall condition with the following settings: "DPM escape" for the spray dryer surface and "reflect" for the pipe wall. The drying air intake speed was 8 m/s, the hydraulic diameter was 0.1351, the turbulence intensity was 3.94, the initial temperature is 100°C, 120°C, 140°C, 160°C, and 180°C, with the mass loading value of 0.0015 kg/s, particle density of 816.4 kg/m^3, and the gas density of 1.225 kg/m^3.

The Rosin-Rammler distribution, which assumes an exponential relationship between particle diameter and proportion of particles, was used to assess particle size distribution (PSD), as shown in Eq. (15) below

$$Y_d = e^{\left(\frac{d}{\bar{d}}\right)^n} \tag{15}$$

where d is the particle size (mm), $\bar{d}$ is the average diameter (mm), and n is the dispersion diameter, calculated according to Eq. (16).

$$n = \frac{ln(-ln\, y_d)}{ln(d/\bar{d})} \tag{16}$$

In this study, the particle diameter ranged from 10 µm to 130 µm in an increment of 20 µm and $\bar{d}$ of 50 µm.

2.4 Numerical Grid and Grid Independence Analysis

Mesh generation was performed based on the element size using ANSYS Mesh. Tetrahedral cell was chosen as the mesh type and the body sizing feature with the curvature size function was added to the meshing of the geometry, which in turn resulted in the adjustment of the element's size according to the shape and size of the geometry. The mesh structure of both spray dryers is presented in Figure 3.

The grid independence analysis was used to forecast the spray dryer's outlet temperature using multiple grid sizes ranging from 0.015 m (coarse mesh) to 0.0135 m (fine mesh) with the same

boundary and operation conditions. Table 3 shows the calculated outlet temperature for different grid sizes. It could be shown that when the grid size was less than 0.0145 m (medium mesh), the simulation results no longer differ. As a result, for all following simulations, a grid size of 0.0145 m was chosen since it provided an acceptable level of grid independence while maintaining a reasonable processing time.

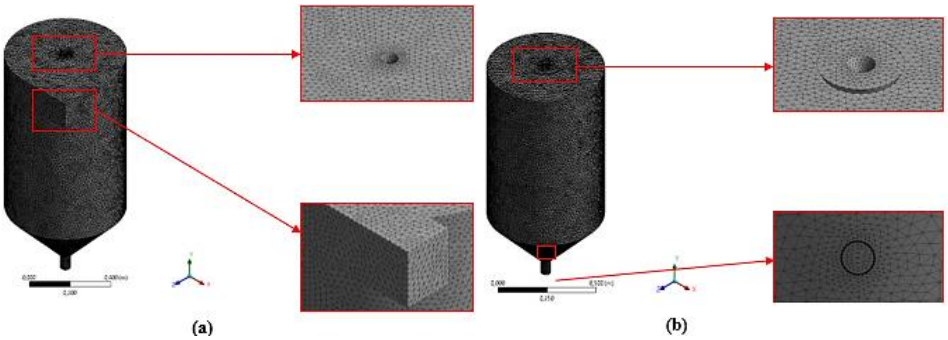

Fig. 3. Mesh structure of (a) mixed flow spray dryer and (b) co-current flow spray dryer

Table 3
Grid independence test results

Cell Size (m)	Outlet Temperature (°C)
0.0130	32.39
0.0135	33.09
0.0140	32.89
0.0145	32.73
0.0150	34.56

2.5 Validation of the Numerical Model

The validation of this study was conducted by comparing the simulation results with the experimental results of research by Habtegebriel *et al.,* [16]. The comparison of outlet temperature and water content between the present model and the published work is presented in Figure 4. The current CFD results for outlet temperature and water content were found to be in good agreement with the reference, with the maximum error being 9.23%. Because the current solver computational settings accurately predicted the exit temperature and water content, the methodology was adopted for all subsequent simulations.

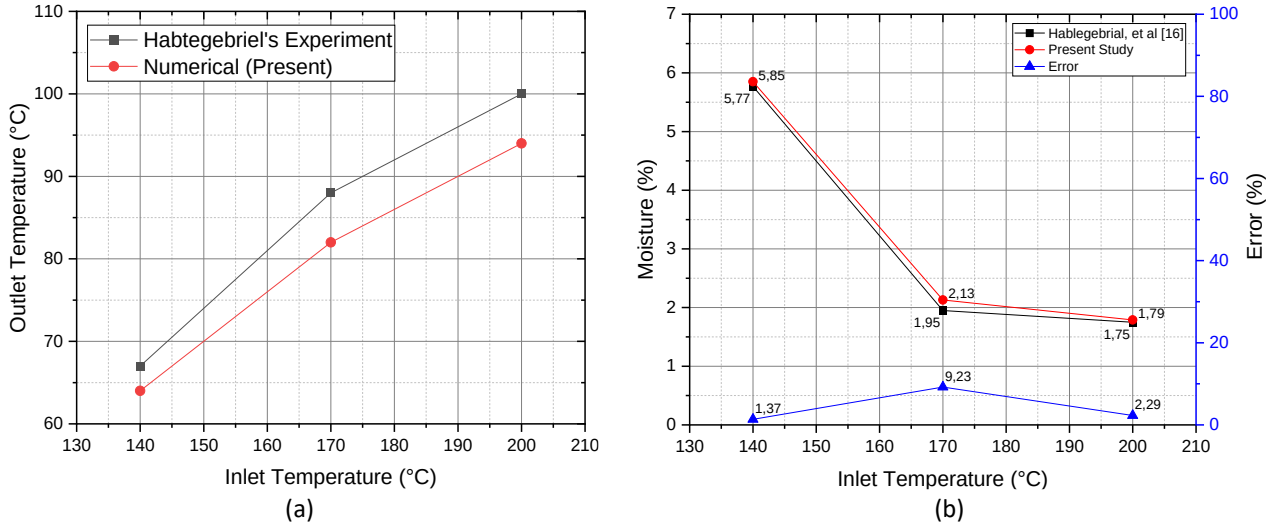

Fig. 4. Comparison of (a) outlet temperature and (b) water content between numerical and experimental results

3. Result and Discussion

3.1 The Effect of Inlet Temperature and Type of Drying Airflow on Water Content

Water content is the water composition in food, with lower water content product is preferred as it is less likely to be contaminated by microbes, thus increasing the quality of the product [32]. Inlet temperature has a big influence on the water content of the dried product, with higher drying air temperature increases the energy of the drying medium. This allows for greater rate of evaporation or mass transfer between the air and the droplets during the drying process, therefore decreasing the water content of the droplets [5,16,32,39-42].

Figure 5 compares the water content in the final dried product between the mixed and co-current flow spray dryer. The droplet diameter of 50 µm is given the emphasize as it is the average droplet diameter in this study that can be useful to compare the performance of both spray dryers. Both mixed and co-current flow spray dryers produced droplets with the lowest water content (0%) at an inlet temperature of 180°C and droplet diameters of 10 µm and 30 µm. The highest water content occurred on droplet diameter of 130 µm with an inlet temperature of 100°C for both mixed flow (58.15%) and co-current flow (59.32%) spray dryers. This trend is in agreement with the result of Obón *et al.,*'s [21] study where the researchers found the water content of particle decreases with inlet temperature of 120°C to 200°C, from 2.9 ± 0.4 % to 2.1 ± 0.2 % for the co-current flow spray dryer and 1.9 ± 0.3 % to 1.6 ± 0.3 % for the mixed flow spray dryer.

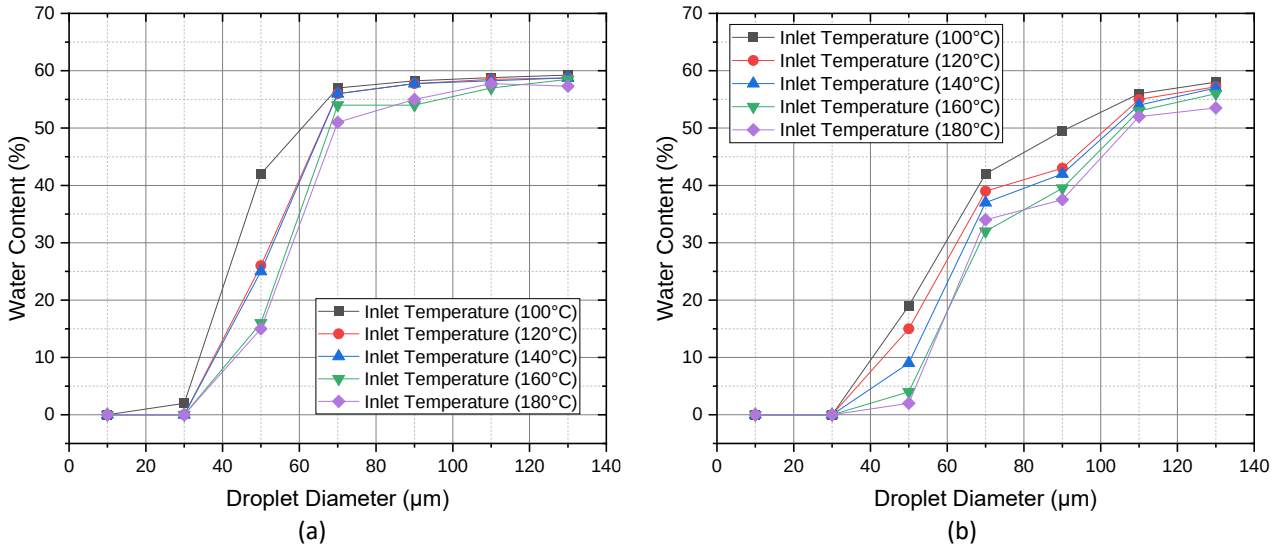

Fig. 5. Comparison of water content in droplets in the drying chamber of (a) mixed flow and (b) co-current flow spray dryers

Both spray dryers showed a linear correlation of droplet diameter and water content in the dried product. Droplets with larger diameters had higher water content than droplets with smaller diameters. This is because droplet diameter significantly influences the rate of mass transfer [1]. The increase in the size of the droplets creates a larger mass and surface area of the particles. This droplet size increase decreases the evaporation rate, thus reducing the mass flow rate between droplets and drying air, resulting in wetter particles [43].

It can be concluded that mixed flow spray dryer produced higher mass flow change than co-current flow dryer, as clearly shown by the lower water content of particles with an average diameter of 50 μm in Figure 5. However, it should be noted that lower water content in powders creates a tendency for the particles to absorb ambient moisture in the storage environment, thereby impairing the stability of the powder in later storage [14]. Careful selection of inlet temperature becomes crucial for the whole production process to ensure the quality of the dried product.

3.2 The Effect of Inlet Temperature and Type of Drying Airflow on Minimum Droplet Temperature

The minimum temperature of particles that exit the spray dryer affects the product quality and post-drying processes. The increase in inlet temperature can increase the minimum temperature of particles that exit the spray dryer [35]. A comparison of minimum droplet temperature produced by both spray dryers is shown in Figure 6. The lowest minimum droplet temperature (32.73°C) was produced by mixed flow spray dryer at an inlet temperature of 100°C. In comparison, the highest one (62.85°C) was produced by co-current flow spray dryer at an inlet temperature of 180°C. This finding is in line with the study of Habtegebriel *et al.,* [16] where moisture content of milk powder decreases dramatically when inlet temperature is raised from 413K to 473K.

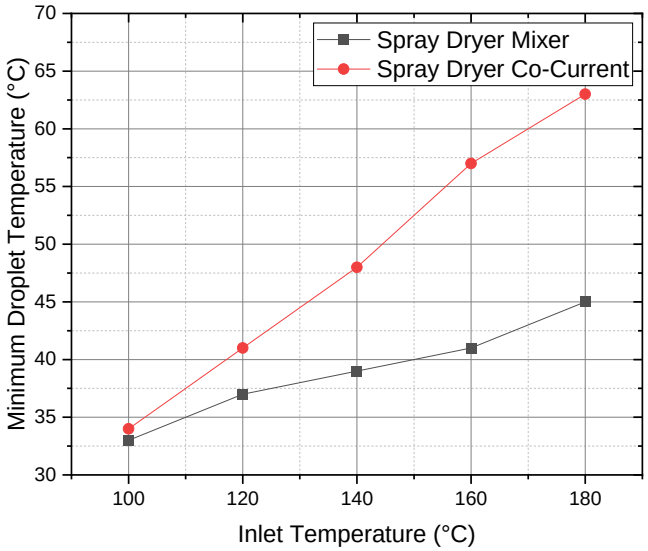

Fig. 6. Comparison of minimum droplet temperature in the drying chamber of mixed flow and co-current flow spray dryer

Overall, it can be seen that mixed flow spray dryer produced droplets with lower minimum droplet temperature compared to co-current flow spray dryer at all inlet temperature variations. Figure 6 that shows the difference in temperature contour and distribution along the radial direction at several elevations for both spray dryers with the highest inlet temperature (180°C). The co-current flow spray dryer produces high-temperature airflow concentrated in the centre of the drying chamber that pushes the droplets directly to the outlet [16]. This phenomenon can be seen in red-boxed area in Figure 7. It is crucial to note that the high minimum droplet temperature produced by high inlet temperature can affect the bioactive compounds on the drying product, in this case, the tea particles. Too high of a drying temperature can result in the loss of polyphenol compounds present in tea particles, which are caused by heat-induced oxidation [14].

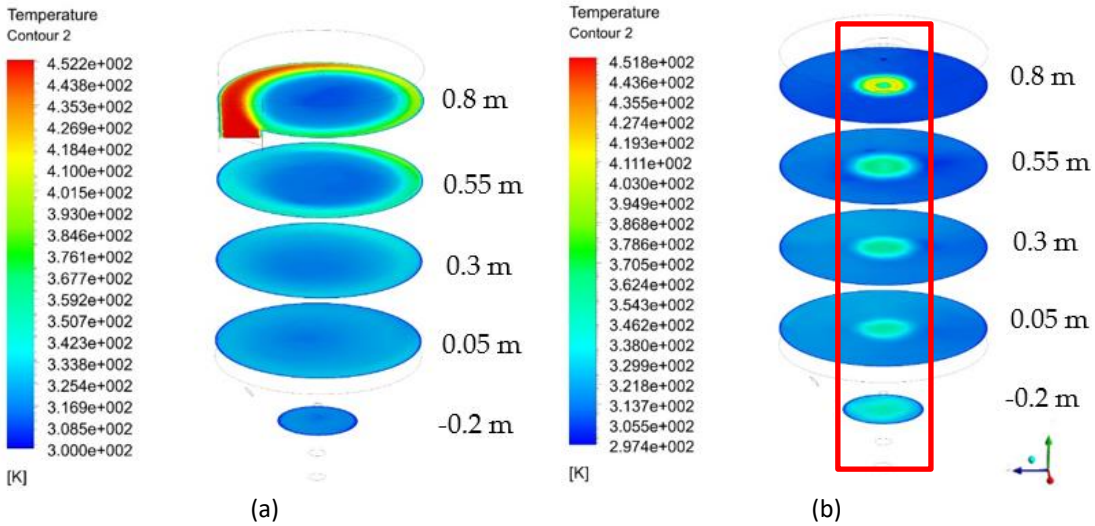

Fig. 7. Temperature contour and distribution at an inlet temperature of 180°C of (a) mixed flow and (b) co-current flow spray dryers

4. Conclusion

This paper presents a study of water content and minimum droplet temperature analysis of spray drying process with inlet temperature and airflow direction variations. From this work, it can be concluded that inlet temperature plays a significant role in water content and minimum droplet temperature of spray drying products. With higher mass flow change, the mixed flow spray dryer produced lower water content and minimum droplet temperature compared to the co-current flow spray dryer. The simulation results have been linked to the importance of preservation of polyphenol compounds in tea leaves and its post-drying processes. Future studies could continue to assess the parameters in choosing the proper inlet temperature for the drying process of tea leaves.

Acknowledgement
This work has initially been accepted and presented at the ICE-SEAM 2021.

References
[1] Anandharamakrishnan, C., Jolius Gimbun, A. G. F. Stapley, and Chris D. Rielly. "A study of particle histories during spray drying using computational fluid dynamic simulations." *Drying Technology* 28, no. 5 (2010): 566-576. https://doi.org/10.1080/07373931003787918
[2] Wang, Yong, and Cordelia Selomulya. "Spray drying strategy for encapsulation of bioactive peptide powders for food applications." *Advanced Powder Technology* 31, no. 1 (2020): 409-415. https://doi.org/10.1016/j.apt.2019.10.034
[3] Salas, Myriam C. Rojas, Héctor J. Ciro Velásquez, and Jesús H. Gil Gonzalez. "Spray drying of sisal liquids extracts (Furcraea spp.): Overall performance of the drying process." *Powder Technology* 321 (2017): 163-172. https://doi.org/10.1016/j.powtec.2017.08.005
[4] Leimann, V. F., Odinei Hess Gonçalves, Guilherme D. Sorita, Stephany Rezende, Evandro Bona, I. P. M. Fernandes, Isabel C. F. R. Ferreira, and M. F. Barreiro. "Heat and pH stable curcumin-based hydrophilic colorants obtained by the solid dispersion technology assisted by spray-drying." *Chemical Engineering Science* 205 (2019): 248-258. https://doi.org/10.1016/j.ces.2019.04.044
[5] Wei, Yucong, Meng Wai Woo, Cordelia Selomulya, Winston Duo Wu, Jie Xiao, and Xiao Dong Chen. "Numerical simulation of mono-disperse droplet spray dryer under the influence of nozzle motion." *Powder Technology* 355 (2019): 93-105. https://doi.org/10.1016/j.powtec.2019.07.017
[6] Uscategui, Diana C. Ruano, Héctor J. Ciro Velásquez, and José U. Sepúlveda Valencia. "Concentrates of sugarcane juice and whey protein: Study of a new powder product obtained by spray drying of their combinations." *Powder Technology* 333 (2018): 429-438. https://doi.org/10.1016/j.powtec.2018.04.025
[7] Saha, Dhritiman, Saroj K. Nanda, and Deep N. Yadav. "Optimization of spray drying process parameters for production of groundnut milk powder." *Powder Technology* 355 (2019): 417-424. https://doi.org/10.1016/j.powtec.2019.07.066
[8] Grosshans, Holger, Matthias Griesing, Thomas Hellwig, Werner Pauer, Hans-Ulrich Moritz, and Eva Gutheil. "A new model for the drying of mannitol-water droplets in hot air above the boiling temperature." *Powder Technology* 297 (2016): 259-265. https://doi.org/10.1016/j.powtec.2016.04.023
[9] Schmitz-Schug, Iris, Ulrich Kulozik, and Petra Foerst. "Modeling spray drying of dairy products-Impact of drying kinetics, reaction kinetics and spray drying conditions on lysine loss." *Chemical Engineering Science* 141 (2016): 315-329. https://doi.org/10.1016/j.ces.2015.11.008
[10] O'Sullivan, Jonathan J., Eve-Anne Norwood, James A. O'Mahony, and Alan L. Kelly. "Atomisation technologies used in spray drying in the dairy industry: A review." *Journal of Food Engineering* 243 (2019): 57-69. https://doi.org/10.1016/j.jfoodeng.2018.08.027
[11] Mhatre, Susmit, Tishya Srivastava, Shivraj Naik, and Vandana Patravale. "Antiviral activity of green tea and black tea polyphenols in prophylaxis and treatment of COVID-19: A review." *Phytomedicine* 85 (2021): 153286. https://doi.org/10.1016/j.phymed.2020.153286
[12] Anjarsari, Intan Ratna Dewi. "Katekin teh Indonesia: prospek dan manfaatnya." *Kultivasi* 15, no. 2 (2016): 99-106. https://doi.org/10.24198/kultivasi.v15i2.11871
[13] Mozumder, N. H. M. Rubel, Kyeong Hwan Hwang, Min-Seuk Lee, Eun-Hee Kim, and Young-Shick Hong. "Metabolomic understanding of the difference between unpruning and pruning cultivation of tea (Camellia sinensis) plants." *Food Research International* 140 (2021): 109978. https://doi.org/10.1016/j.foodres.2020.109978

[14] Thi Anh Dao, Dong, Hoang Van Thanh, Do Viet Ha, and Vuong Duc Nguyen. "Optimization of spray-drying process to manufacture green tea powder and its characters." *Food Science & Nutrition* 9, no. 12 (2021): 6566-6574. https://doi.org/10.1002/fsn3.2597

[15] Warjito, Warjito, Sanjaya B. S. Nasution, Muhammad Farhan Syahputra, Budiarso Budiarso, and Dendy Adanta. "Study of turbulence model for performance and flow field prediction of pico hydro types propeller turbine." *CFD Letters* 12, no. 8 (2020): 26-34. https://doi.org/10.37934/cfdl.12.8.2634

[16] Habtegebriel, Haileeyesus, Dintwa Edward, Oboetswe Motsamai, Michael Wawire, Eyassu Seifu, and Sila Daniel. "The potential of computational fluid dynamics simulation to investigate the relation between quality parameters and outlet temperature during spray drying of camel milk." *Drying Technology* 39, no. 13 (2021): 2010-2024. https://doi.org/10.1080/07373937.2019.1684317

[17] Benavides-Morán, Aldo, Alfonso Cubillos, and Alexánder Gómez. "Spray drying experiments and CFD simulation of guava juice formulation." *Drying Technology* 39, no. 4 (2021): 450-465. https://doi.org/10.1080/07373937.2019.1708382

[18] Kavoshi, Leila, Amir Rahimi, and Mohammad Sadegh Hatamipour. "CFD modeling and experimental study of carbon dioxide removal in a lab-scale spray dryer." *Chemical Engineering Research and Design* 98 (2015): 157-167. https://doi.org/10.1016/j.cherd.2015.04.023

[19] Hussain, Farooq, Maciej Jaskulski, Marcin Piatkowski, and Evangelos Tsotsas. "CFD simulation of agglomeration and coalescence in spray dryer." *Chemical Engineering Science* 247 (2022): 117064. https://doi.org/10.1016/j.ces.2021.117064

[20] Filková, Iva, and Arun S. Mujumdar. "Industrial spray drying systems." In *Handbook of Industrial Drying*, pp. 263-307. CRC Press, 2020. https://doi.org/10.1201/9780429289774-9

[21] Obón, J. M., J. P. Luna-Abad, B. Bermejo, and J. A. Fernández-López. "Thermographic studies of cocurrent and mixed flow spray drying of heat sensitive bioactive compounds." *Journal of Food Engineering* 268 (2020): 109745. https://doi.org/10.1016/j.jfoodeng.2019.109745

[22] Zhang, Tao, and Bi-Botti C. Youan. "Analysis of process parameters affecting spray-dried oily core nanocapsules using factorial design." *AAPS PharmSciTech* 11, no. 3 (2010): 1422-1431. https://doi.org/10.1208/s12249-010-9516-7

[23] Fazaeli, Mahboubeh, Zahra Emam-Djomeh, Ahmad Kalbasi Ashtari, and Mahmoud Omid. "Effect of spray drying conditions and feed composition on the physical properties of black mulberry juice powder." *Food and Bioproducts Processing* 90, no. 4 (2012): 667-675. https://doi.org/10.1016/j.fbp.2012.04.006

[24] Julklang, Wittaya, and Boris Golman. "Effect of process parameters on energy performance of spray drying with exhaust air heat recovery for production of high value particles." *Applied Energy* 151 (2015): 285-295. https://doi.org/10.1016/j.apenergy.2015.04.069

[25] Jubaer, Hasan, Sepideh Afshar, Jie Xiao, Xiao Dong Chen, Cordelia Selomulya, and Meng Wai Woo. "On the effect of turbulence models on CFD simulations of a counter-current spray drying process." *Chemical Engineering Research and Design* 141 (2019): 592-607. https://doi.org/10.1016/j.cherd.2018.11.024

[26] Jubaer, Hasan, Sepideh Afshar, Guénolé Le Maout, Serge Mejean, Cordelia Selomulya, Jie Xiao, Xiao Dong Chen, Romain Jeantet, and Meng Wai Woo. "The impact of self-sustained oscillations on particle residence time in a commercial scale spray dryer." *Powder Technology* 360 (2020): 1177-1191. https://doi.org/10.1016/j.powtec.2019.11.023

[27] Liu, Yuyang, Yu Rao, and Bernhard Weigand. "Heat transfer and pressure loss characteristics in a swirl cooling tube with dimples on the tube inner surface." *International Journal of Heat and Mass Transfer* 128 (2019): 54-65. https://doi.org/10.1016/j.ijheatmasstransfer.2018.08.097

[28] Sadripour, Maryam, Amir Rahimi, and Mohammad Sadegh Hatamipour. "Experimental study and CFD modeling of wall deposition in a spray dryer." *Drying Technology* 30, no. 6 (2012): 574-582. https://doi.org/10.1080/07373937.2011.653613

[29] Mezhericher, M., A. Levy, and I. Borde. "Droplet-droplet interactions in spray drying by using 2D computational fluid dynamics." *Drying Technology* 26, no. 3 (2008): 265-282. https://doi.org/10.1080/07373930801897523

[30] Jaskulski, M., J. C. Atuonwu, T. T. H. Tran, A. G. F. Stapley, and E. Tsotsas. "Predictive CFD modeling of whey protein denaturation in skim milk spray drying powder production." *Advanced Powder Technology* 28, no. 12 (2017): 3140-3147. https://doi.org/10.1016/j.apt.2017.09.026

[31] Topcu, Okan. "CFD-DP Modelling of Multiphase Flow in Dense Medium Cyclone." *CFD Letters* 4, no. 1 (2012): 33-42.

[32] Arepally, Divyasree, and Tridib Kumar Goswami. "Effect of inlet air temperature and gum Arabic concentration on encapsulation of probiotics by spray drying." *LWT* 99 (2019): 583-593. https://doi.org/10.1016/j.lwt.2018.10.022

[33] Roustapour, Omid Reza, Mostafa Hosseinalipour, Barat Ghobadian, Fazlolah Mohaghegh, and Neda Maftoon Azad. "A proposed numerical-experimental method for drying kinetics in a spray dryer." *Journal of Food Engineering* 90, no. 1 (2009): 20-26. https://doi.org/10.1016/j.jfoodeng.2008.05.031

[34] Aguirre-Alonso, R. O., M. Morales-Guillermo, M. A. Salgado-Cervantes, V. J. Robles-Olvera, M. A. García-Alvarado, and G. C. Rodríguez-Jimenes. "Effect of process variables of spray drying employing heat pump and nitrogen on aromatic compound yield in powders obtained from vanilla (Vanilla planifolia Andrews) ethanolic extract." *Drying Technology* 37, no. 14 (2019): 1806-1820. https://doi.org/10.1080/07373937.2018.1540011

[35] Langrish, T. A. G., and R. Premarajah. "Antioxidant capacity of spray-dried plant extracts: Experiments and simulations." *Advanced Powder Technology* 24, no. 4 (2013): 771-779. https://doi.org/10.1016/j.apt.2013.03.020

[36] Tan, Yaoyao, Yue Zhao, Honghai Hu, Nan Fu, Chunjiang Zhang, Hong Zhang, and Xiaofeng Dai. "Drying kinetics and particle formation of potato powder during spray drying probed by microrheology and single droplet drying." *Food Research International (Ottawa, Ont.)* 116 (2019): 483-491. https://doi.org/10.1016/j.foodres.2018.08.064

[37] Morsi, S. A. J., and A. J. Alexander. "An investigation of particle trajectories in two-phase flow systems." *Journal of Fluid Mechanics* 55, no. 2 (1972): 193-208. https://doi.org/10.1017/S0022112072001806

[38] Masilungan-Manuel, Joanna Tess, Mark Christian E. Manuel, Po Ting Lin, and Allan N. Soriano. "Optimization of the drying parameters for the short-form spray dryer producing powdered egg with 20% tapioca starch additive." *Advances in Mechanical Engineering* 7, no. 9 (2015): 1687814015602603. https://doi.org/10.1177/1687814015602603

[39] Both, E. M., R. M. Boom, and M. A. I. Schutyser. "Particle morphology and powder properties during spray drying of maltodextrin and whey protein mixtures." *Powder Technology* 363 (2020): 519-524. https://doi.org/10.1016/j.powtec.2020.01.001

[40] Sablania, Vandana, and Sowriappan John Don Bosco. "Optimization of spray drying parameters for Murraya koenigii (Linn) leaves extract using response surface methodology." *Powder Technology* 335 (2018): 35-41. https://doi.org/10.1016/j.powtec.2018.05.009

[41] Pui, L. P., R. Karim, Y. A. Yusof, C. W. Wong, and H. M. Ghazali. "Optimization of spray-drying parameters for the production of 'Cempedak'(Artocarpus integer) fruit powder." *Journal of Food Measurement and Characterization* 14, no. 6 (2020): 3238-3249. https://doi.org/10.1007/s11694-020-00565-3

[42] Gouaou, Imen, Samira Shamaei, Mohamed Salah Koutchoukali, Mohamed Bouhelassa, Evangelos Tsotsas, and Abdolreza Kharaghani. "Impact of operating conditions on a single droplet and spray drying of hydroxypropylated pea starch: Process performance and final powder properties." *Asia-Pacific Journal of Chemical Engineering* 14, no. 1 (2019): e2268. https://doi.org/10.1002/apj.2268

[43] de Oliveira, Aparecida Helena, Mario Eduardo R. M. Cavalcanti Mata, Mauri Fortes, Maria Elita Martins Duarte, Matheus Pasquali, and Hugo M. Lisboa. "Influence of spray drying conditions on the properties of whole goat milk." *Drying Technology* 39, no. 6 (2021): 726-737. https://doi.org/10.1080/07373937.2020.1714647